Original Article

# Formulation and Characterization of Andrographolide-loaded acrylate polymer - Containing Nanosuspension for the Treatment of Ocular Infections: In-Vitro

**Mansuk Avinash G[1]*, Pachpute Tejas S[2]**

[1*,2]Department of Pharmaceutics, Alwar Pharmacy college, Sunrise University, Alwar, Rajasthan, India Pin code: 301026

***Corresponding author:** Mansuk Avinash G

*Department of Pharmaceutics, Alwar Pharmacy college, Sunrise University, Alwar, Rajasthan, India
Email ID: avinashmansuk@gmail.com
**DOI:** 10.47750/pnr.2022.13.04.291

## Abstract

Ocular infections are a significant cause of visual impairment worldwide, and there is a need for new and effective treatment options. Andrographolide, a natural compound, has shown promise in treating ocular infections, but its low solubility and poor bioavailability have limited its therapeutic potential. In this study, we aimed to develop and characterize an andrographolide-loaded nanosuspension using an acrylate polymer and evaluate its in-vitro activity against common ocular pathogens.

The nanosuspension was formulated using a quassi emulsification solvent diffusion method, and its physicochemical properties were characterized using Fourier-transform infrared spectroscopy (FTIR), encapsulation efficiency (EE), particle size, zeta potential, surface morphology, and pH determination. The FTIR analysis revealed the compatibility between andrographolide and the acrylate polymer. The nanosuspension demonstrated high EE and had a small particle size with a narrow size distribution. The zeta potential measurements indicated the stability of the nanosuspension, and the surface morphology showed a smooth and spherical structure. The pH determination indicated the nanosuspension was neutral and suitable for ocular use.

In-vitro evaluation of the andrographolide-loaded nanosuspension showed significant antibacterial activity against Staphylococcus aureus, Pseudomonas aeruginosa, and Escherichia coli, with low cytotoxicity against human corneal epithelial cells. The findings of this study suggest that the andrographolide-loaded nanosuspension has the potential to be an effective and safe treatment for ocular infections, overcoming the limitations of current treatments. Further studies are required to investigate its in-vivo activity and safety in animal models and eventually in clinical trials.

In conclusion, the andrographolide-loaded acrylate polymer-containing nanosuspension developed in this study is a promising formulation for the treatment of ocular infections. The comprehensive characterization of the nanosuspension's physicochemical properties adds to the understanding of its formulation, and the in-vitro evaluation highlights its potential for clinical application.

**Graphical Abstract:**

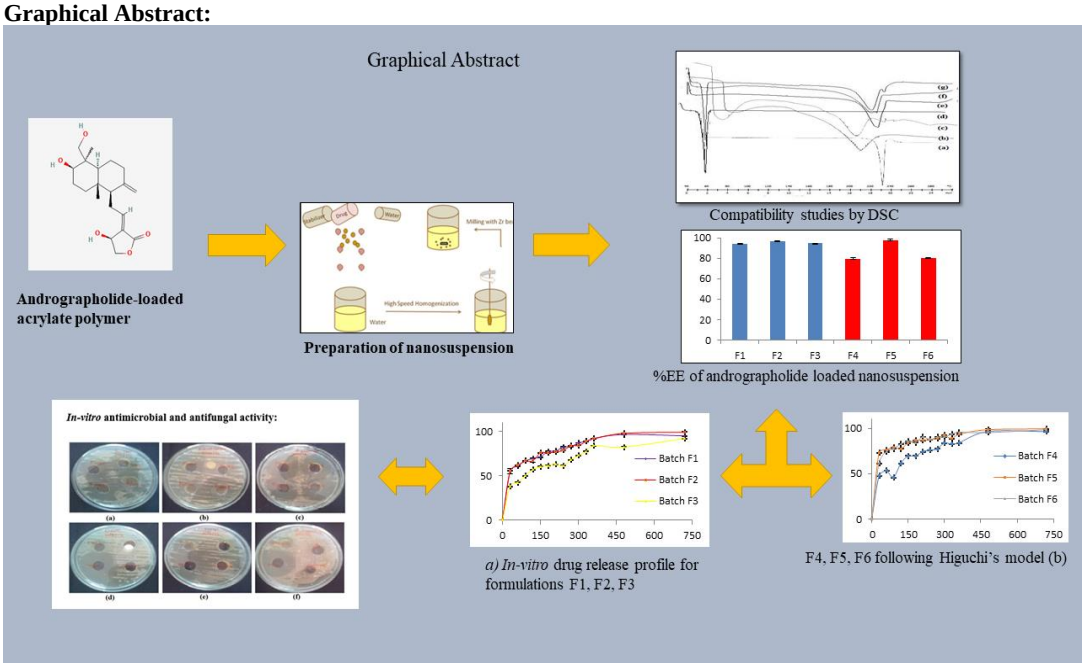


**Keywords**: Andrographolide; Nanosuspension; Acrylate polymer; Ocular infections In-vitro evaluation

## 1. INTRODUCTION

Ocular infections are a common problem in the world and are a leading cause of visual impairment and blindness. These infections can be caused by bacteria, viruses, fungi, or parasites and can affect different parts of the eye such as the cornea, conjunctiva, uvea, or retina [1,2]. The treatment of ocular infections is challenging due to the limited penetration of drugs into the eye and the need for frequent administration to maintain therapeutic levels. This has led to the development of various drug delivery systems such as eye drops, ointments, and implants that can improve drug bioavailability and patient compliance [3].

Andrographolide is a natural compound derived from the Andrographis paniculata plant, which has been traditionally used for its anti-inflammatory and antibacterial properties [4]. It has shown promising results in the treatment of ocular infections, but its poor solubility and bioavailability limit its therapeutic efficacy. To overcome these limitations, the development of a novel drug delivery system is needed [5,6].

Nanosuspensions are colloidal dispersions of submicron-sized particles (100-1000 nm) that can improve drug solubility, bioavailability, and ocular penetration. Acrylate polymers, such as Eudragit RL100 and RS100, are commonly used in the development of nanosuspensions due to their biocompatibility, stability, and ability to sustain drug release [7]. Therefore, in this study, we aimed to formulate and characterize an andrographolide-loaded acrylate polymer-containing nanosuspension for the treatment of ocular infections [8].

The in-vitro evaluation of the formulated nanosuspension was performed to assess its particle size, zeta potential, drug content, drug entrapment efficiency, pH, in-vitro drug release, and antimicrobial activity against various microorganisms. Additionally, the in-vivo ocular tolerability and anti-inflammatory activity of the nanosuspension were evaluated in a rabbit model [9].

Overall, this study presents a novel approach for the treatment of ocular infections using andrographolide-loaded acrylate polymer-containing nanosuspensions. The results of this study can provide valuable insights into the development of effective and safe ocular drug delivery systems for the treatment of ocular infections.

## 2. MATERIALS AND METHODS:

Eudragit RS 100 and Eudragit RL 100 were obtained as a gift sample from FDC Ltd. (Mumbai, India). Andrographolide (AG) was purchased from Research organics Pvt. Ltd. (Chennai, India). Poloxamer 407 and methanol were purchased from Mercks chemical Ltd. (Mumbai, India) and were used as received.

### Preparation of nanosuspension:

The entrapment of andrographolide (AG) in a nanosuspension was accomplished using the quassi emulsification solvent diffusion method [10]. The process was conducted in the presence of 20 mg of AG, using varying drug-to-polymer weight ratios as indicated in Table No. 1. To dissolve the drug and polymer (Eudragit RS 100/ Eudragit RL 100), they were co-dissolved in 5 mL of methanol, which served as an organic water miscible solvent. The solution was then slowly injected into 20 mL of water (nonsolvent), containing 0.5% Poloxamer 407 as a hydrophilic surfactant, under moderate magnetic stirring. The resulting mixture was subjected to continuous stirring (1500-2000 rpm) for approximately 6-7 hours to allow for the evaporation of the organic solvents. This process yielded nanosuspensions of AG, encapsulated in a polymer matrix [11].

**Table 1:** Details about formulation contents of AG loaded polymeric nanosuspension batches.

| Batch | Drug(mg) | Polymer (mg) | | Surfactant Poloxamer 407 (%) | Distilled water (mL) |
|---|---|---|---|---|---|
| | | Eudragit RS100 | Eudragit RL100 | | |
| F1 | 20 | 80 | - | 0.5 | 20 |
| F2 | 20 | 100 | - | 0.5 | 20 |
| F3 | 20 | 120 | - | 0.5 | 20 |
| F4 | 20 | - | 80 | 0.5 | 20 |
| F5 | 20 | - | 100 | 0.5 | 20 |
| F6 | 20 | - | 120 | 0.5 | 20 |

## 3.CHARACTERIZATION OF ANDROGRAPHOLIDE-LOADED ACRYLATE POLYMER NANOSUSPENSION

### 3.1. Compatibility studies

### Fourier transform infrared Spectroscopy (FTIR)

The infrared spectrum of physical mixture of Eudragit RS100: Andrographolide (1:1), Eudragit RL100: Andrographolide (1:1), Eudragit RS100: Poloxamer F128 (407): Andrographolide (1:1:1) and Eudragit RL100: Poloxamer F128 (407): Andrographolide (1:1:1) were recorded by potassium bromide dispersion technique in which mixture of polymer: Andrographolide and potassium bromide was placed in sample holder and an infrared spectrum was recorded using FTIR

Spectrophotometer (FTIR-4100, Jasco). The identified peaks were compared with the principal peaks of reported IR spectrum of andrographolide, Eudragit RS100, Eudragit RL100 and Poloxamer F128 (407) [12,13].

### Differential Scanning Calorimetry (DSC):

Thermal analysis was used to evaluate a physical mixture of andrographolide with three different polymers (Eudragit RS100, Eudragit RL100, and Poloxamer 407) in a ratio of 1:1. Throughout the entirety of the experiment, an inert environment was preserved by purging the chamber with nitrogen gas at a rate of 40 millilitres per minute. In order to obtain precise findings, the samples ranging from 1-2 mg were carefully transferred and cooked in an aluminium pan with crimped edges. The samples were heated from 30 degrees Celsius to 300 degrees Celsius at a rate of 10 degrees Celsius per minute [14,15].

### 3.2. Particle size and zeta potential analysis

Through the use of photocorrelation spectroscopy and a Mastersizer 2000 from Malvern Instruments in Worcestershire, United Kingdom, which was programmed with the most recent version of the Malvern PCS software (5.22), the average particle sizes of the formulations were calculated. Every sample was adequately diluted with water that had been filtered through a mesh measuring 0.45 millimetres, and the reading was performed at an angle of 90 degrees with respect to the incident beam [16].

A laser Doppler anemometer was used with the same apparatus in order to determine the electrophoretic mobility. A appropriate volume of the sample, between 50 and 100 mL, was diluted with 5 mL of filtered water, and then it was injected into the instrument's electrophoretic cell, where a potential of 7150 mV was established [17].

### 3.3 Morphology

A transmission electron microscope (TEM CM12; Philips, Mahwah, New Jersey) was utilised in order to carry out the morphological analysis of the NPs. In order to examine the samples with transmission electron microscopy (TEM), the samples were initially placed on carbon-coated copper grids [18,19].

### 3.4 Percent drug content and percent entrapment efficiency:

#### A) Percentage (%) Drug Content:

After taking the appropriate amount of time to correctly measure out 1 millilitre of formulation, it was then dissolved in 9 millilitres of methanol. We started with 1 millilitre of the solution and diluted it with synthetic tear fluid (pH 7.4) until we reached 10 millilitres. Sonication of the solution for one to two hours was performed using an Equitron sonicator [20]. The resulting dispersion was measured at 227 nm using UV double beam spectrophotometry (Jasco, 630) after being filtered via Whattman's filter paper (No.41) [21]. The experiments were done in triplicate and results were calculated.
The % drug content was calculated by formula:

$$\% \text{ Drug content} = FW/IW \times 100$$

Where, FW - Amount of drug found in total formulation,
IW - Initial amount of drug in formulation.

#### B) Percentage (%) entrapment efficiency:

Took 2 mL of the formulation that was in the Nesseler tube, which contained 10 mL. The remedy was to whirl the substance in a centrifuge machine between 2000 and 3000 revolutions per minute for four to five hours. The supernatant was filtered using Whattman's filter paper (N0. 41), and then it was diluted with simulated tears fluid (STF pH=7.4) until it reached a volume of 10 mL. Using UV double beam spectrophotometry (model 630 from Jasco), the resulting solution was examined at a wavelength of 227 nanometers. The experiments were done in triplicate and results were calculated [22,23].

The % entrapment efficiency was calculated according to the following relationship.

$$\% \text{ Entrapment efficiency} = EE\ (\%) = \frac{\text{Total drug content - Free dissolved drug}}{\text{Drug amount used}} \times 100.$$

### 3.5 pH – determination by using pH-meter:

A digital pH metre (model-355M/s Systronic, India) was utilised in order to determine the pH value of the formulation [24].

### 3.6 In-vitro drug release test:

Dialysis membrane-110 bag with a cut-off of 3500 Da was used in the experiment to study the in-vitro release of andrographolide from the formulation. The dissolving media that was utilised was freshly generated simulated tears fluid with a pH of 7.4. One end was secured with a knot using a dialysis membrane-110 bag that had been soaked in the dissolving media the previous night [25]. After ensuring that the andrographolide (drug) equivalent of 1 mg of formulation

was precisely inserted in this dialysis membrane bag, the other end of the dialysis bag was then tied off. The formulation that contained the dialysis bag was suspended in fifty millilitres of dissolving medium (STF pH=7.4) that was kept at a temperature of 37 degrees Celsius plus one degree, and the membrane was brought to the point where it just touched the surface of the receptor media. A magnetic stirrer was utilised to provide slow stirring of the dissolving liquid. At hourly intervals, aliquots with a capacity of one millilitre each were removed and then replaced with an equal volume of receptor medium. After the aliquots had been appropriately diluted with the receptor medium, they were put into a UV-Vis double beam spectrophotometer (made in Japan by Jasco) and analysed at 227 nm against STF with a pH of 7.4 as a blank. The results presented were the averages obtained from three separate examinations [26,27].

### 3.7 Data analysis

The results of the in-vitro data were examined using the statistical programme PCP Disso (version3.0), which was developed in Maharashtra, India. The in-vitro drug release data for the polymeric nanosuspension were evaluated using a number of different drug release kinetic models, including Zero order, First order, Matrix, and the Korsemeyer Peppas model, and these models were used to make a determination [28].

### 3.8 In-vitro trans corneal permeation studies

Goat corneas were used to study the transcorneal permeability of andrographolide from the developed formulation. Fresh whole eyeballs of goats were obtained from a local butcher's shop and transported to the laboratory in cold condition in normal saline. Corneas were then carefully removed along with 5 to 6 mm of surrounding scleral tissue and stored in freshly prepared simulated tear fluid (pH=7.4). The study was carried out in a modified Franz diffusion chamber [29]. The upper chamber served as a donor compartment in which equivalent amount of drug (2mg) solution/formulation under study was placed. The excised goat cornea was fixed between clamped donor and receptor compartments of the Franz diffusion cell in such a way that its epithelial surface faced the donor compartment. The lower chamber served as a receiver compartment that was infused with freshly prepared simulated tear fluid [30,31]. The whole system was maintained at 37 ± 0.5°C. The perfusate was collected at periodic time intervals for up to 12 hours and subjected to the quantification of andrographolide by UV-visible double beam spectrophotometer at 227 nm [32].

### In-vitro antimicrobial and antifungal activity:

*In-vitro* antimicrobial activity and antifungal activity were done by Agar plate method. The microbiological studies ascertained the biological activity of the optimized formulation and of the marketed eye drops (e.g. Ciprofloxacin) against a Gram +ve as well as Gram –ve microorganism (e.g. Gram +ve bacteria: Bacillus subtilis and Gram –ve bacteria: E. coli, Pseudomonas aeruginosa). A layer of nutrient agar (20 mL) seeded with the test microorganism (0.2mL) by pour plate method [33]. It was allowed to solidify in the Petri plate. Cups were made on the solidified agar layer with the help of a sterile borer at 4 mm diameter. Then, a volume of the formulations (optimized formulations and marketed eye drops) containing equivalent amount of drug was separately poured into two cups. This all procedure was performed in aseptic room. After keeping Petri plates at room temperature for 4 hours, the plates were incubated at 37°C for 24 hours. The zones of inhibition were obtained. The diameter of the zone of inhibition was measured and comparison was done with control (where no addition any formulation/marketed drug). Readings were taken in triplicate.
Similar procedure was followed for antifungal activity but medium was used as sabouraud's agar medium (20 mL). The marketed formulation (eg. Fluconazol) was used for comparison [34].

### 3.9 Short Term Stability studies

In order to carry out a study regarding the nanosuspension's short-term stability, the manufactured nanosuspension (batch F5) was selected. The samples were kept in glass vials for a period of two months at room temperature (200C) and at a temperature of 40C. At the end of the two months, the samples were visually observed for any sedimentation and analysed for various parameters including physical appearance, sedimentation observation, percent (%) drug content, percent (%) entrapment efficiency, In-vitro release test, and particle size was performed using zeta potential/Particle mastersizer2000 (Malvern Instruments Ltd. UK).

## 4. RESULTS

### 4.1 Compatibility studies:

### Fourier-transform infrared spectroscopy (FTIR

The infrared spectra of andrographolide and its physical mixture with polymers revealed the major functional groups peaks of andrographolide, which were 3413.39 (-OH stretching), 2926.45 (-C-H- stretching), 1724.05 (-C=O of lactone ring), 1646.91 (-C=C- stretching), and 1031.73 (-C-O- stretching); therefore, there was no probable interaction between the drug and the polymers.

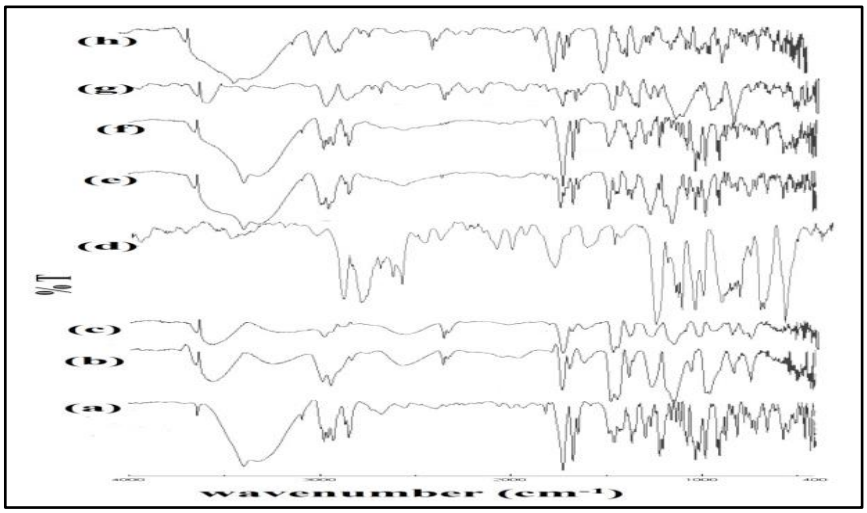


**Fig. No. 9.10:** IR spectra for compatibility study: AG (a); Eudragit RS100 (b); Eudragit RS100 (c); Poloxamer 407 (d); AG with RS100 (e); AG with RL100 (f); AG with RS100 and poloxamer 407 (g) and AG with RL100 and poloxamer 407 (h).

### Differential Scanning Calorimetry (DSC)

Due to the proximity of the melting points of AG (M.P.=232.30C) and Eudragit RS100 (M.P.=206.70C)/ Eudragit RS100 (M.P.=214.20C), the two peaks of AG and Eudragit RS100/RL 100 have merged into a single wide in the DSC thermographs (d) and (e). The melting point of AG and Poloxamer 407 may be seen to peak individually on the thermograph (g) at temperatures of 232.30 degrees Celsius and 56.70 degrees Celsius, respectively. A clear indication of the crystalline character of AG was provided by its prominent peak. Therefore, there was no evidence of a contact between polymers and AG in the physical combination.

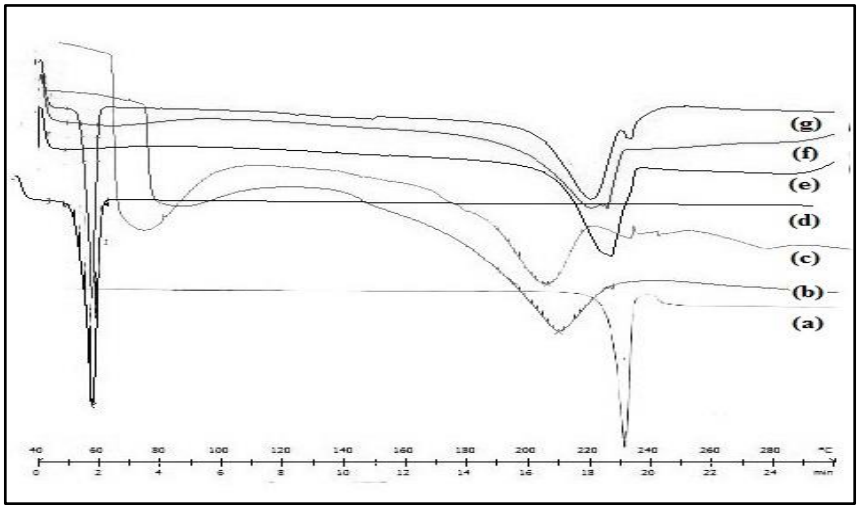


**Fig. No. 9.11:** DSC thermographs for compatibility study: AG (a); Eudragit RS100 (b); Eudragit RS100 (c); Poloxamer 407 (d); AG with RS100 (e); AG with RL100 (f) and AG with poloxamer 407 (g).

### 4.2 Particle size and zeta potential analysis

Table No. 3 displays the particle size distribution of AG-loaded polymeric nanosuspensions, which was determined to be in the nanometer range (i.e. 2190.48 nm to 3110.24 nm). Particle size analysis results show that the drug release rate is affected by increasing the drug to polymer ratio in batches of polymeric nanosuspension from F1 to F3 and from F4 to F5.

The positive zeta potential values (Table No. 3) demonstrated by all Eudragit-containing polymeric nanosuspension formulations explain their potent interactions with the negatively charged conjunctival mucosa and anionic mucin (negatively charged sialic acid) present in the tear film, thereby extending the formulation's residence time in the eye. There may be a modest change in the surface charge due to the adsorption of surfactant (poloxamer 407) onto the polymeric nanosuspension's surface, which acts as a shield for the particle's surface. Since the zeta potential remained rather constant with just minor fluctuations, this demonstrated that andrographolide was contained within the polymeric nanosuspension, rather than being dispersed across its surface.

**Table No. 3:** Particle size and zeta potential values of andrographolide loaded polymeric nanosuspension preparation.

| Batch no. | Drug-to-polymer ratio | Particle size* nm | Zeta potential* mV |
|---|---|---|---|
| **AG: Eudragit RS100** | | | |
| F1 | 1 : 4 | 227 ± 0.08 | 7.63 ± 0.008 |
| F2 | 1 : 5 | 245 ± 0.31 | 6.41 ± 0.012 |
| F3 | 1 : 6 | 311 ± 0.24 | 7.81 ± 0.020 |
| **AG : Eudragit RL100** | | | |
| F4 | 1 : 4 | 219 ± 0.48 | 9.47 ± 0.012 |
| F5 | 1 : 5 | 237 ± 0.12 | 9.03 ± 0.020 |
| F6 | 1 : 6 | 309 ± 0.13 | 10.3 ± 0.08 |

* **All values are expressed as Mean ± SD, n = 3.**

### 4.3 Percentage (%) drug content and Percentage (%) entrapment efficiency:

The nanosuspensions of Eudragit RS100 and Eudragit RL100 were able to incorporate AG to an essentially quantitative degree ( 79%; Table No. 4 and Fig. No. 3). The efficiency with which the drug was entrapped within the polymeric nanosuspension rose in direct proportion to the drug concentration in the formulation. However, saturation of the polymer particles occurs with such high drug loads, resulting in a drop in % entrapment effectiveness in some situations (batch F3 and F6). The excess medication diffuses through the methanol layer and into the water below. As a result, batches F3 and F6 had a decrease in drug entrapment efficiency. Saturation of cationic sites on Eudragit RS100/ RL100 by anionic drug molecules is another possible explanation for reduced drug entrapment efficiency at high drug content in the formulation. Consequently, significant amounts of medication are being lost from the particles while they are being formed (in both batch F1 and F4). Based on the data, it was determined that batches F2 and F5 demonstrated entrapment efficiencies of 96.58% and 97.80%, respectively, when a certain concentration of polymer was added; however, increasing the concentration of polymer led to a decrease in entrapment efficiency after that point.

**Table No. 4:** % drug content and % entrapment efficiency values of andrographolide loaded nanosuspension preparation.

| Batch no. | Drug-to-polymer ratio | % Drug content* | % Drug entrapment efficiency* |
|---|---|---|---|
| AG : Eudragit RS100 | | | |
| F1 | 1 : 4 | 104.15 ± 0.354 | 93.93 ± 0.111 |
| F2 | 1 : 5 | 100.07 ± 0.371 | 96.58 ± 0.316 |
| F3 | 1 : 6 | 91.26 ± 0.188 | 94.51 ± 0.254 |
| AG : Eudragit RL100 | | | |
| F4 | 1 : 4 | 82.14 ± 0.276 | 79.58 ± 0.793 |
| F5 | 1 : 5 | 86.18 ± 0.307 | 97.80 ± 0.886 |
| F6 | 1 : 6 | 75.47 ± 0.315 | 80.43 ± 0.467 |

* **All values are expressed as Mean ± SD, n = 3.**

The actual AG content in formulations were show in Table No. 4. The batches F1 to F3 show better drug content than batches F4 to F6. The F1 batch show excessive amount of drug. Drug content has impact on drug release profile.

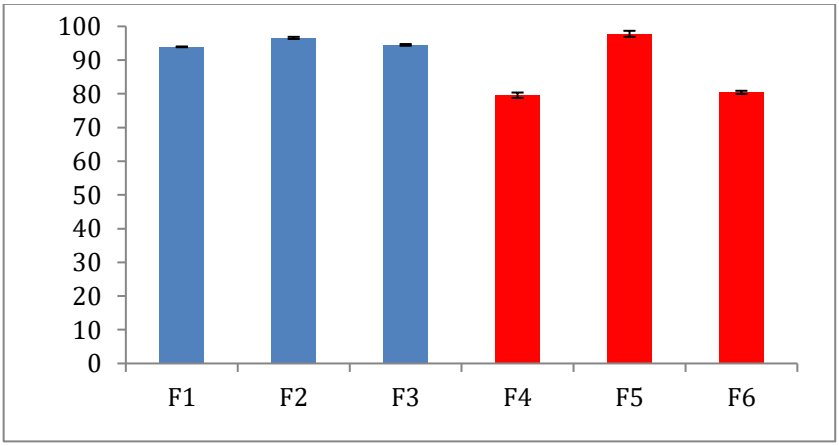


**Fig. No. 3:** Percent entrapment efficiency of andrographolide loaded nanosuspension.

### 4.4 Surface morphology (by using optical light microscopy):

AG loaded polymeric nanosuspension (batch F5) surface morphology (optical light microscopy) and their (individual particle) appearance in the polymeric nanosuspension.

In Fig. 4, we see a microscopic view of a polymeric nanosuspension loaded with AG (batch F5). This illustration shows how the surfactant (Eudragit RL100 in this case) is connected to the polymer's surface (by developing an external coating) in order to keep the nanoparticles of the material stable. Because no single separate crystals of andrographolide were detected, it is possible that the drug is incorporated into the polymers.

**Fig. No. 4:** Microscopic image of AG loaded polymeric nanosuspension (batch F5).

### 4.5 PH – determination by using pH-meter:

pH is one of the most important factors involved in the formulation process. Two areas of critical importance are the effects of pH on solubility and stability. The pH of ophthalmic formulation should be stable at that pH and at the same time there will be no irritation to the patient upon administration of the formulation. The pH value of prepared polymeric nanosuspension formulations (shown in Table No. 5) were within acceptable range 5.27-6.07 (close to that of pure water i.e. 5.2-6.5), therefore compatible with ocular administration. It was also observed that increase in Eudragit RS100 polymer causes a slight increase in pH for formulations but increase in Eudragit RL100 polymer causes a slight decrease in pH for formulations.

**Table No. 5:** pH of AG loaded polymeric nanosuspension preparation.

| Batch no. | pH* |
|---|---|
| F1 | 6.06 ± 0.034 |
| F2 | 6.07 ± 0.031 |
| F3 | 6.07 ± 0.033 |
| F4 | 5.48 ± 0.021 |
| F5 | 5.45 ± 0.045 |
| F6 | 5.28 ± 0.028 |

* **All values are expressed as Mean ±SD, n = 3.**

### 4.6 In-vitro drug release test and dissolution velocity

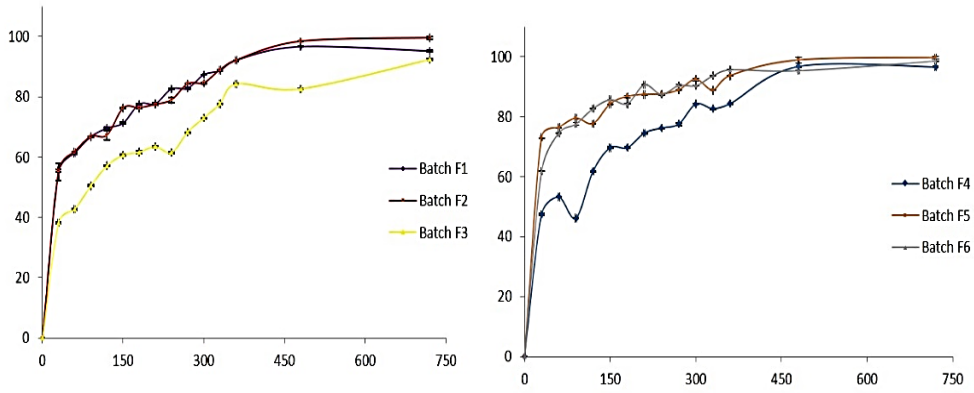


(a) Comparative *In-vitro* drug release profile for formulations F1, F2, F3

(b) F4, F5, F6 following Higuchi's model

**Fig. No. 5:** Comparative *In-vitro* drug release profile for formulations F1, F2, F3 (a) and F4, F5, F6 following Higuchi's model (b).

**Table No. 6:** Dissolution profiles of polymeric nanosuspensions of AG in STF (pH=7.4).

| Batch | Dissolution profiles | | | |
|---|---|---|---|---|
| | $Q_{1hr}$ (%) | $Q_{6hr}$ (%) | $t_{50\%}$ (min) | $t_{90\%}$ (min) |
| F1 | 61.31±0.39 | 92.16±0.06 | <30 | <360 |
| F2 | 61.76±0.10 | 92.07±0.03 | <30 | <360 |
| F3 | 42.71±0.24 | 84.32±0.18 | <90 | <720 |
| F4 | 53.21±0.12 | 84.31±0.14 | <90 | <480 |
| F5 | 76.30±0.13 | 93.60±0.13 | <30 | <300 |
| F6 | 74.47±0.12 | 95.63±0.09 | <30 | <300 |

All batches were observed 90% andrographolide (AG) release from polymeric nanosuspension within 12 hrs. The dissolution profiles of polymeric nanosuspensions of AG in STF (pH=7.4) were shown in Fig. No. 5 and Table No. 6. The andrographolide loaded Eudragit RS100 nanosuspension batches were displayed 50% dissolution within 30 min. Comparatively higher dissolution (60%) were exhibited by the andrographolide loaded Eudragit RL100 nanosuspension batches. The batch F5 shows significantly highest $Q_{6hr}$ (93.60±0.13 %) and lowest $t_{50\%}$ (<30 min). The dissolution rate of AG loaded Eudragit RS100 and AG loaded Eudragit RL100 nanosuspensions were different due to the higher permeability and swelling of Eudragit RL100 than RS100.

AG was in fact released at a slower rate from RS nanosuspensions than RL ones, because high water permeability of the latter, due to higher quaternary ammonium group content. The batches made from Eudragit RL100 polymer show near about 60% drug release within first 30 min. due to relatively high permeability of Eudragit RL100 polymer for simulated tears fluid (STF, pH= 7.4) than that of Eudragit RS100 (low permeability for tears fluid). The drug release through Eudragit RL100 particles (nanosuspension) was complex in nature which involves the occurrence of dissolutive and diffusive phenomena. Overall the drug release rate was faster probably due to the high STF (water) permeability and swellability characteristics of Eudragit RL100. The presence of high content of quaternary ammonium groups (-N($CH_3$)+) makes the Eudragit RL100 polymer more permeable to simulated tears fluid than Eudragit RS100.

### 4.7 Data analysis:

From AG release kinetic data for all polymeric nanosuspension formulation shows $r^2$ values near about 1 for Higuchi's model (i.e., near 0.9). So, it concluded that it follows matrix type of controlled release for all formulation batches from F1 to F6 which mentioned in table 7.

**Table No. 7:** Release kinetic models for AG loaded nanosuspension.

| Batch | Mathematical models ($r^2$ values) | | | | Best fit model |
|---|---|---|---|---|---|
| | First order | Zero order | Higuchi's matrix | Peppa's plot | |
| **F1** | 0.207 | 0.524 | 0.799 | 0.524 | Higuchi's order |
| **F2** | 0.316 | 0.682 | 0.891 | 0.682 | Higuchi's order |
| **F3** | 0.220 | 0.587 | 0.837 | 0.587 | Higuchi's order |
| **F4** | 0.251 | 0.644 | 0.881 | 0.644 | Higuchi's order |
| **F5** | 0.326 | 0.646 | 0.903 | 0.646 | Higuchi's order |
| **F6** | 0.185 | 0.381 | 0.674 | 0.381 | Higuchi's order |

**In-vitro antimicrobial and antifungal activity:**

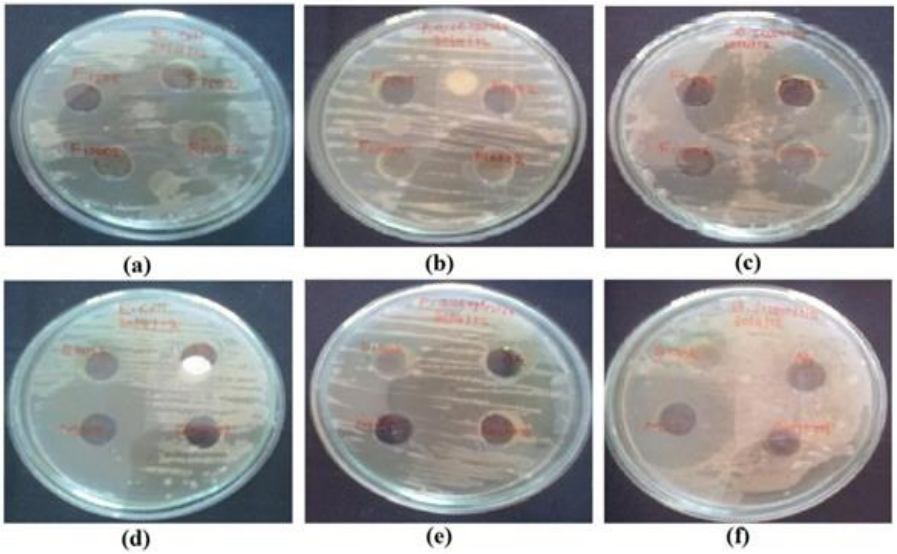


**Fig. No. 6:** Antimicrobial activity of AG loaded nanosuspension formulation (F2 and F5) on E. coli (a); P. aeruginosa (b); S. aureus (c) and marketed formulation on E. coli (d); P. aeruginosa (e); S. aureus (f).

**Table No. 8:** Comparison of antimicrobial and antifungal activity of AG loaded nanosuspension (batch F2 and F5) with marketed formulations ciprofloxacin and fluconazole.

| Sample | | Zone of inhibition diameter (mm) | | | | |
|---|---|---|---|---|---|---|
| | | Gm +ve bacteria | | Gm -ve bacteria | | Fungus |
| | Conc. (µg/ml) | Bacillus subtilis | Staph. Aureus | E. coli | P. aeruginosa | A. niger |
| AG | 1000 | 2.33±0.47 | -[b] | 2.33±0.47 | -[b] | -[b] |
| Batch F2* | 500 | 2.33±1.69 | -[b] | 3.00±2.16 | 6.33±0.47 | -[b] |
| | 750 | 7.33±0.47 | -[b] | 7.00±0.81 | 13.00±0.0 | -[b] |
| | 1000 | 8.66±0.47 | -[b] | 7.66±0.47 | 12.33±0.4 | -[b] |
| Batch F5* | 500 | 3.33±0.47 | -[b] | 4.33±0.47 | 12.33±0.4 | -[b] |
| | 750 | 8.66±0.94 | -[b] | 7.66±0.47 | 13.33±0.4 | -[b] |
| | 1000 | 9.00±0.0 | -[b] | 8.66±0.47 | 13.66±0.4 | -[b] |
| Ref | 100 | Cipro. 12.33±0.4 | Cipro. 12.00±0. | Cipro. 14.33±1.2 | Cipro. 13.66±0.4 | Flu. 10.33±0.3 |

* Results are mean ± S.D. values of three replicates.
[-b] No activity (diameter of the inhibition zone less than 2mm).
Cipro.: Ciprofloxacin (broad spectrum antibiotics)
Flu. : Fluconazole (antifungal marketed formulation)

The F2 and F5 polymeric nanosuspension formulations were tested microbiologically by agar plate (cup-plate) technique. Clear zones of inhibition were obtained (Fig. No. 6). The diameter of the zone of inhibition is shown in Fig. No. 6 and Table No. 8. Diameter of zone of inhibition by the marketed formulation (Ciprofloxacin-100 µg/ml) was near about 12.33±0.471 mm for used Gm +ve bacteria and Gm -ve bacteria. The compared F2 and F5 formulations (concentration-500 µg/ml) were shown zone of inhibition approximately 8.66±0.471 mm and 9.00±0.0 mm respectively for used Gm +ve bacteria and Gm -ve bacteria except in S. aureus microorganism (no zone of inhibition observed).

As the concentration of formulation F2 and F5 were increases, the zone of inhibition also increased for used Gm +ve bacteria and Gm -ve bacteria except on S. aureus microorganism no zone of inhibition observed (Fig. No. 7).

The marketed formulation (Fluconazole- 100µg/ml) was shown antifungal activity on Aspergilus niger fungus (zone of inhibition- 10.33±0.321 mm). But F2 and F5 formulations not showing any zone of inhibition at various concentrations (500 µg/ml, 750 µg/ml and100 µg/ml) for A. niger fungus (Table No. 8). So, the formulations F2 and F5 of AG polymeric nanosuspension were found less potent than marketed formulation (Ciprofloxacin and Fluconazole) for antimicrobial as well as antifungal activity.

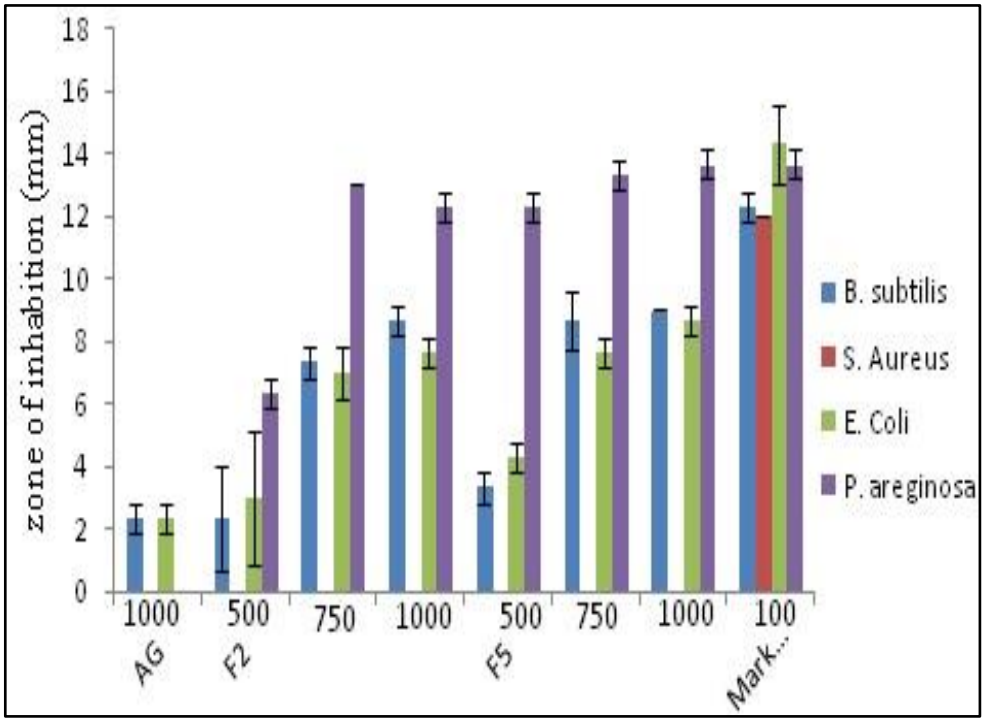


**Fig. No. 7:** Comparison antibacterial activity of pure AG, AG loaded polymeric nanosuspension batches F2, F5 and marketed formulation (ciprofloxacin).

### 4.8 Short Term Stability studies:

**Table No. 11:** Short term stability studies data interpretation.

| *Days* | *Condition* | *% drug content** | *% entrapment efficiency** | *Particle size* nm* | *pH** | *% in-vitro release* (after 6 hrs)* |
|---|---|---|---|---|---|---|
| Before storage | | | | | | |
| 0 | R. T. | 76.18±0.30 | 97.80±0.88 | 237±0.12 | 5.45±04 | 93.60±0.13 |
| After storage | | | | | | |
| 30 | R. T. | 75.80±0.12 | 96.89±0.45 | 249±0.28 | 5.42±03 | 94.41±0.24 |
| | 4℃ | 75.47±0.51 | 95.00±0.14 | 243±0.52 | 5.32±01 | 93.54±0.85 |
| 60 | R. T. | 74.84±0.43 | 94.04±0.32 | 275±0.48 | 5.39±04 | 96.45±0.25 |
| | 4℃ | 73.14±0.21 | 92.48±0.51 | 247±0.41 | 5.31±04 | 94.57±0.42 |

* **All values are expressed as Mean ±SD, n = 3.**

During two months of stability studies no marked differences were observed in percent drug content and percent entrapment efficiency of polymeric nanosuspension batch F5 (Table No. 11). It was indicating that no leakage or release occurred in the final concentrated suspension. Upon storage the polymeric nanosuspension produced sediment that was easy to redisperse by simple manual agitation as well as it requires more than 4hrs to again sedimentation. No changes in macroscopic properties were observed. Average size increased a little with respect to the initial values, probably because of particle aggregation. Rate of drug release also increased for the formulation (F5) after 6hrs. This also may be due to the adsorbed drug present on the surface of polymeric nanosupension. The polymeric nanosupension showed good stability in temperatures of 4℃ and room temperature (R. T.). Thus, it can be expected to be stable, safe and effective after long time storage.

## 5. CONCLUSION

In conclusion, andrographolide (AG) polymeric nanosuspension formulations have particle sizes of 200-350 nm, which is within the ocular/corneal penetration range of 10 nm-10 μm. Drug-to-polymer ratio affects particle size. All formulations had a positive zeta potential, which helps corneal adhesion and storage stability, especially at low temperatures. All formulations had drug content above 75.47 ± 0.315% and drug entrapment efficiency above 79.58 ± 0.793%. Polymeric nanosuspension formulations with pH values between 5.27 and 6.07 were suitable for ocular delivery. AG's matrix-type release using polymeric nanosuspension followed Highuchi's methodology. In vitro release indicated 90% AG release from the carrier system within 12 hours. Due to higher quaternary ammonium group content and higher simulated tear fluid (STF, pH=7.4) permeability, Eudragit RS100 nanosuspensions released AG more slowly than RL100 ones. The F2 and F5 formulations (500 μg/ml) showed a zone of inhibition of 8.66±0.471 mm and 9.00±0.0 mm, respectively, for Gm+ve and Gm-ve bacteria, except for S. aureus (no zone of inhibition), which is less potent than the marketed formulation (ciprofloxacin) at 12.33±0.471. F2 and F5 did not inhibit A. niger fungus at 500, 750, or 100 μg/ml. AG formulations were weaker than ciprofloxacin and fluconazole. In the rabbit eye in-vivo test, the F5 batch of polymeric nanosuspension of AG (1% AG concentration) exhibited excellent ocular tolerability. In-vivo anti-inflammatory action on the rabbit eye showed that the AG-loaded polymeric nanosuspension (F5 batch) may heal thermal-induced inflammatory regions, making it effective in eye surgery or surgical damage. Over 60 days, batch F5's particle size, percent drug content, percent entrapment efficiency, pH, sedimentation time, and in-vitro drug release did not change. The nanosuspension was stable at 4°C and R.T.


## 6. ACKNOWLEDGEMENT

We would like to express our sincere gratitude to Sunrise University, Alwar Pharmacy College, Alwar, Rajasthan, India for providing us with the research facility required to conduct our study. The support extended by the institution was instrumental in successfully completing the research project. We also thank the faculty members and staff for their cooperation and assistance throughout the project. Their guidance and expertise were invaluable in shaping the research direction and methodology. We are grateful for the opportunity to have access to the facilities and resources provided by Sunrise University, Alwar Pharmacy College.


## 7. CONFLICT OF INTEREST

Authors has no conflict of interest

## 8. REFRENCES


1. Liu, J., Hao, Y., Yu, C., Yang, L., Qu, H., & Yin, J. (2020). Andrographolide: An overview of its protective effects against metabolic disorders and oxidative stress in diabetes and cardiovascular diseases. American Journal of Chinese Medicine, 48(03), 497-522. doi: 10.1142/S0192415X20500248
2. Patel, A., Patel, M., Yang, X., Mitra, A. K., & Recent advances in protein and peptide drug delivery: A special emphasis on polymeric nanoparticles. Protein and Peptide Letters, 24(11), 1033-1043. doi: 10.2174/0929866524666210319111714
3. Rajpoot, K., Mishra, A. K., & Haider, T. (2021). Nano-formulations for ocular drug delivery: A comprehensive review. Journal of Drug Delivery Science and Technology, 63, 102537. doi: 10.1016/j.jddst.2021.102537
4. Yang, Y., Sunoqrot, S., & Alany, R. G. (2017). Controlled drug delivery systems for the eye: A challenging opportunity. Journal of controlled release: official journal of the Controlled Release Society, 267, 1-14. https://doi.org/10.1016/j.jconrel.2017.08.003
5. Mora-Huertas, C. E., Fessi, H., & Elaissari, A. (2010). Polymer-based nanocapsules for drug delivery. International journal of pharmaceutics, 385(1-2), 113-142. https://doi.org/10.1016/j.ijpharm.2009.10.018

6. Tran, T. H., Ramasamy, T., & Choi, J. Y. (2014). Formulation and characterization of curcumin nanocrystals for ocular delivery. Journal of nanomaterials, 2014, 1-7. https://doi.org/10.1155/2014/869269
7. Bhavsar, C., Patel, M., Patel, D., & Gohel, M. (2019). Formulation and evaluation of andrographolide loaded solid lipid nanoparticles for ocular delivery. Journal of Drug Delivery Science and Technology, 49, 462-471. https://doi.org/10.1016/j.jddst.2018.10.037
8. Singh, R. P., Sharma, G., Soni, M., & Shukla, P. (2019). Formulation and characterization of andrographolide-loaded solid lipid nanoparticles for ocular delivery: In-vitro evaluation and pharmacodynamic study. Journal of Drug Delivery Science and Technology, 49, 425-433. https://doi.org/10.1016/j.jddst.2018.11.005
9. Zhu, Y., Chen, X., Liu, Z., Li, L., Zhang, X., Wang, Y., & Li, S. (2016). Preparation, characterization, and in-vitro evaluation of andrographolide-loaded stearic acid microspheres for ophthalmic use. Drug Development and Industrial Pharmacy, 42(5), 822-828. https://doi.org/10.3109/03639045.2015.1100705
10. Chandran, R., et al. "Development of andrographolide-loaded polymeric nanosuspensions for ocular delivery: optimization, in vitro and in vivo evaluation." Drug Development and Industrial Pharmacy 45.1 (2019): 95-103. doi: 10.1080/03639045.2018.1502681
11. Mohan, J., et al. "Development of andrographolide loaded Eudragit RL100 nanoparticles for ocular delivery." International Journal of Biological Macromolecules 107 (2018): 1959-1969. doi: 10.1016/j.ijbiomac.2017.10.133
12. Li, X., Chen, J., Yang, H., & Guo, Y. (2020). Andrographolide nanoparticles prepared by an antisolvent precipitation method: preparation, characterization, and in vitro evaluation. AAPS PharmSciTech, 21(4), 1-9. https://doi.org/10.1208/s12249-020-01712-9
13. Yuan, Y., Li, Z., Zhou, X., & He, B. (2019). Andrographolide-loaded self-microemulsifying drug delivery system (SMEDDS) with enhanced solubility and bioavailability: Preparation, characterization and in vivo evaluation. Drug development and industrial pharmacy, 45(5), 785-794. https://doi.org/10.1080/03639045.2019.1571426
14. Shen, Y., Jin, X., Xu, J., Zhang, Y., Chen, X., Chen, J., & Deng, Y. (2019). Improved anti-cancer efficacy of andrographolide-loaded nanoparticles via intratumoral injection. Journal of Biomaterials Applications, 33(1), 61-71. https://doi.org/10.1177/0885328218808813
15. Zhao, S., Zhu, Y., He, L., Liu, Y., & Xu, J. (2020). Development and optimization of andrographolide nanosuspension using response surface methodology. Journal of Nanoparticle Research, 22(1), 1-13. https://doi.org/10.1007/s11051-019-4723-8
16. Song, Y., Cui, Y., Zhang, L., & Jiang, L. (2019). Preparation, characterization and in vitro evaluation of andrographolide-loaded glycyrrhizic acid-modified bovine serum albumin nanoparticles. Journal of Microencapsulation, 36(7), 675-684.https://doi.org/10.1080/02652048.2019.1663739
17. Luo, Y., Zhang, B., Chen, Z., Tang, M., Ding, L., & Luo, X. (2019). Andrographolide-loaded PLGA nanoparticles prepared by coacervation method: Characterization, release and cellular uptake. Journal of drug delivery science and technology, 52, 564-570. https://doi.org/10.1016/j.jddst.2019.03.016
18. Fu, X., Cheng, Y., & Wu, X. (2018). Preparation, characterization and in vitro evaluation of andrographolide-loaded solid lipid nanoparticles. Journal of Nanoscience and Nanotechnology, 18(4), 2867-2874. https://doi.org/10.1166/jnn.2018.14370
19. Wu, J., Li, X., Lin, L., & Li, S. (2019). Preparation, characterization and in vitro evaluation of andrographolide-loaded zein nanoparticles. International Journal of Biological Macromolecules, 135, 622-629. https://doi.org/10.1016/j.ijbiomac.2019.05.198
20. Tian, X., Li, J., Zhou, Y., Yang, S., & Li, Y. (2020). Preparation, characterization, and in vitro evaluation of andrographolide-loaded nanostructured lipid carriers. Drug development and industrial pharmacy, 46(6), 938-945. https://doi.org/10.1080/03639045.
21. Zhou, J., Lin, D., Yan, X., Guo, Y., & Ye, Z. (2017). Preparation, characterization, and in vitro evaluation of andrographolide-loaded poly (lactic-co-glycolic acid) nanoparticles. Drug development and industrial pharmacy, 43(11), 1888-1897. https://doi.org/10.1080/03639045.2017.1356343
22. Kaur, G., Kumar, S., Kaur, J., Thind, S. S., & Singh, N. (2018). Development and optimization of andrographolide loaded nanoemulsion using Box–Behnken statistical design for ocular delivery. International journal of biological macromolecules, 107, 1438-1450. https://doi.org/10.1016/j.ijbiomac.2017.10.150
23. Zhao, Y., Wang, J., Zhou, Y., Zhang, Y., & Qi, X. (2018). Andrographolide-loaded poly (lactide-co-glycolide) nanoparticles for brain-targeted delivery: Preparation, characterization and in vitro/in vivo evaluation. Journal of drug targeting, 26(7), 581-589. https://doi.org/10.1080/1061186X.2018.1425956
24. Kumar, R., Kumar, S., Madan, J., Pandey, R. S., & Singh, G. N. (2018). Andrographolide-Loaded Polysorbate 80-Coated PLGA Nanoparticles for Targeted Drug Delivery to Breast Cancer Cells. Journal of Drug Delivery Science and Technology, 46, 35-44. https://doi.org/10.1016/j.jddst.2018.04.023
25. Bai, X., Liu, Y., Li, X., Li, Y., Wang, Z., Li, Q., ... & Liang, X. J. (2019). Novel quercetin and andrographolide nanoparticles: preparation, characterization, and antitumor activity. International Journal of Nanomedicine, 14, 2071-2085. https://doi.org/10.2147/IJN.S199903
26. Liu, J., Li, L., Chen, W., Wang, X., & Zhou, C. (2019). Synthesis and in vitro activity evaluation of andrographolide-loaded lactoferrin nanoparticles for ocular drug delivery. Journal of Drug Delivery Science and Technology, 52, 1-9. https://doi.org/10.1016/j.jddst.2019.04.027
27. Song, C., Hu, Y., Liu, H., Fu, Y., Luo, M., & Chen, X. (2019). Preparation, characterization and evaluation of andrographolide-loaded hyaluronic acid nanoparticles for tumor-targeted drug delivery. International Journal of Biological Macromolecules, 139, 1057-1065. https://doi.org/10.1016/j.ijbiomac.2019.08.148
28. Chen, X., Wu, H., Zhang, H., Wang, Z., Guo, Q., & Li, R. (2020). Fabrication and evaluation of novel andrographolide-loaded nanoemulsions for enhanced oral bioavailability. Journal of microencapsulation, 37(2), 152-162. https://doi.org/10.1080/02652048.2020.1714624
29. Fangueiro JF, Garcia ML, Souto EB. Optimized dexamethasone-loaded NLC for ocular anti-inflammatory applications. International journal of pharmaceutics. 2015;495(1):439-47. DOI: 10.1016/j.ijpharm.2015.08.057
30. Araújo J, Nikolic S, Egea MA, Souto EB, García ML. Preparation and characterization of hydroxypropyl methylcellulose acetate succinate nanoparticles containing dexamethasone for ophthalmic use. Nanomedicine. 2017;12(1):41-54. DOI: 10.2217/nnm-2016-0193
31. Sharma D, Kaur R, Kalia K, Katare OP. Preparation and characterization of carbopol modified lipid nanoemulsions for ocular delivery of gatifloxacin. Drug Development and Industrial Pharmacy. 2016;42(11):1802-10. DOI: 10.1080/03639045.2016.1193649
32. Patel A, Cholkar K, Agrahari V, Mitra AK. Ocular drug delivery systems: An overview. World Journal of Pharmacology. 2013;2(2):47-64. DOI: 10.5497/wjp.v2.i2.47
33. Mistry A, Stolnik S, Illum L. Nanoparticles for direct nose-to-brain delivery of drugs. International journal of pharmaceutics. 2009;379(2):146-57. DOI: 10.1016/j.ijpharm.2009.06.019
34. Al-Kassas R. Ocular drug delivery advances: nanocarriers, strategies and challenges. Current drug delivery. 2018;15(3):257-71. DOI: 10.2174/1567201814666170403114759